Magnesium Technology 2011
Edited by: Wim H. Sillekens, Sean R. Agnew, Neale R. Neelameggham, and Suveen N. Mathaudhu
TMS (The Minerals, Metals & Materials Society), 2011

Macrostructure evolution in directionally solidified Mg-RE alloys

M.A. Salgado-Ordorica, W. Punessen, S. Yi, J. Bohlen, K.U. Kainer and N. Hort

GKSS-Forschungszentrum, Max-Planck-Strasse 1, 21502 Geesthacht, Germany.

Keywords: Magnesium alloys, rare earths, directional solidification, microstructure.

Abstract

The use of Rare-Earths (RE) to develop new cast- and wrought-magnesium alloys has acquired increased interest in recent years. The good mechanical properties of Mg-RE alloys at room temperature, and in particular their high strength at relatively high temperatures are at present well-known facts that make them very promising materials for transport applications. In this context, it is necessary to achieve a better understanding of the macro and microstructure evolution of cast Mg-metals directionally solidified. To this end, binary Mg-RE alloys (where RE = Gd, Nd and Y) were cast by permanent mould direct chill casting. This process was performed in a specially optimized laboratory-scale installation in order to ensure the obtention of "clean" ingots, with homogeneous composition and free of porosity and inclusions. A set of different processing conditions was evaluated in order to better control the final microstructure, mainly in terms of grain size, orientation and distribution. The grain selection mechanisms operating during the solidification of these specimens, namely texturization and Columnar to Equiaxed Transition (CET), were characterized and put into relation with the initial composition of the alloy and the imposed cooling conditions.

Introduction

The characteristics of Rare Earths (RE) and their potential effects when added to Mg melts have been characterized during the last 60 years (1). However, due to new technological developments on RE extraction and separation, it has been only until recently that Mg-RE alloys haver acquired new interest for well defined applications, in particular in transport industry and bio-medical developments. The use of RE in Mg-alloys increase notably their properties at relatively high temperatures (2; 3) and due to their promising role in automotive and aircraft applications, it is important to know at which extent their microstructure evolution can be controlled either in as-cast products or wrought materials.

Chill Casting (CC) of Mg-alloys present a number of complications related to the melt preparation and atmosphere protection. In particular during melting and pouring into the mould, the molten metal can react with air and burn or create oxide layers that will eventually be detrimental to the homogeneity of the final product. Due to volume limitations on the mould size, permanent mould CC has only be applied at a laboratory scale, but the solidified ingots can be further processed to fullfill other requirements.

Other than in die-casting processes, the as-cast microstructure of simple Mg-RE alloys has been poorly investigated and focus has been mainly directed to understand the effect of these alloying elements in further processing stages. In the context of Mg-alloys directionally solidified, some work has been devoted to measure and understand the dendrite growth directions and texture development, in particular in AZ and AM alloys. These studies have shown that there is a strong dependence of the microstructure on the processing conditions, i.e., imposed thermal gradient G and solidification velocity v_s, and the intrinsic properties of the alloy, in particular the solid-liquid interfacial energy $\gamma_{s\ell}$ anisotropy. A pioneer effort on characterizing the microstructure of an AZ91 alloy was performed by Pettersen et al (4; 5). They found that in these alloys, a $\langle 11\bar{2}0\rangle$ texture evolves in specimens directionally solidified at a low G/v_s ratio ($\approx 48/0.32 = 150$ K/s), whereas at $G/v_s \approx 10/0.053 \approx 190$ K/s the texture evolves along a $\langle 22\bar{4}5\rangle$ direction, which is of course not contained within the basal plane. In the first case, the columnar trunks appear bonded by three secondary arms growing at 60 deg. from the trunk, while in the second case two arms belong also to $\langle 22\bar{4}5\rangle$ directions, at 35 deg. from the trunk, and a third one grow along a $\langle 11\bar{2}0\rangle$ direction, at 54 deg. from the trunk. Mirkovic and Fetzer (6) performed also Bridgman solidification experiments and measured primary and secondary arm spacings of AZ31 and AM50 dendritic structures. They also found the growth of a primary trunk with three secondary arms growing at 60 deg. from it. These later observations were further investigated by Eiken et al. and compared to numerical predictions of dendrite growth using the phase-field

method (7). In order to compare simulations and experimental observations, not only the processing conditions were taken into account, but also an appropriate form for the anisotropy of the solid-liquid interfacial energy $\gamma_{s\ell}(\mathbf{n})$ for an hexagonal system was considered. The dependency of $\gamma_{s\ell}$ with respect to the crystallographic orientation, expressed as a vector $\mathbf{n}$ normal to the solid liquid interface in the crystallographic reference frame, was constructed through mathematical functions, called spherical harmonics, that included the two- and six-fold symmetries of an hexagonal system. These simulations reproduced well the texture evolution for dendrites growing along $\langle 11\bar{2}0 \rangle$ directions only in the range of $G/v_s \leq 150K/s$. However, it has been stated in this and other works (8; 9) that for non-basal growth directions, the use of a more complex function of $\gamma_{s\ell}(\mathbf{n})$, might be necessary.

The present work first describes a reliable process to cast Mg-RE ingots of very good quality. A comparison of different solidification conditions for these alloys is presented in order to establish a range of parameters that will allow to control the final microstructure. Finally, an analysis of texture evolution is presented, in particular for Mg-10wt.%Gd alloys.

Experiments and Methods

Alloys preparation

Different binary Mg-RE alloys, where RE = 4wt.%Y, 10wt.%Gd and 2wt.%Nd, were prepared from their pure elements (purity of 99.99%) in a resistances furnace able to heat up a stainless steel crucible of 8 kg capacity. Mg ingots of about 750 g were first molten in the furnace at 720°C, then the corresponding alloying element was added in small quantities not bigger than a few hundreds of grams. After a waiting time of 5 minutes, a six-blade boronitride coated stainless steel propeller, turning at 150 rpm during 30 min, was used to stir the melt and ensure complete mixing. A constant flux of an Ar-SF_6 mixture (in a ratio 5:1) was introduced to the furnace during the whole melting and stirring times, in order to reduce oxidation and burning of the melt. After stirring, oxides remaining on the upper surface of the melt were cleaned out with a boronitride coated stainless steel paddle. The temperature before pouring into the permanent mould was of 700°C.

Permanent mould chill casting

This process has been developed in order to produce, at a laboratory scale, Mg-RE ingots of good quality, free of porosity, with homogeneous composition and controlled microstructure. A schematic representation of the experimental set-up can be observed in Fig. 1a. A three-zones resistances furnace having a tubular shape is bounded in the upper and bottom parts by well-insulated opening hatches. The permanent mould, fabricated with stainless steel and coated in its inner surface with a thin layer of boronitride, was preheated into the tubular furnace at a temperature of 650°C during 15 to 20 min. After pre-heating, the mould was extracted from the tubular furnace through the upper hatch and fixed to a support where the melting furnace could directly fill it. A smooth flux of Ar was passed through the furnace nozzle in order to avoid oxidation and burning of the molten metal during this stage. After pouring, the mould was introduced again into the tubular furnace through the upper hatch and it was covered with a thin steel deck. A secondary flux of an Ar-SF_6 mixture was flowing through the deck in order to keep the atmosphere above the molten metal free of oxygen. Additionally, a 1 mm diameter thermocouple was introduced into a boronitride coated stainless steel capillary tube (3 mm diameter), that was in direct contact with the melt, at about 50 mm from the bottom of the mould.

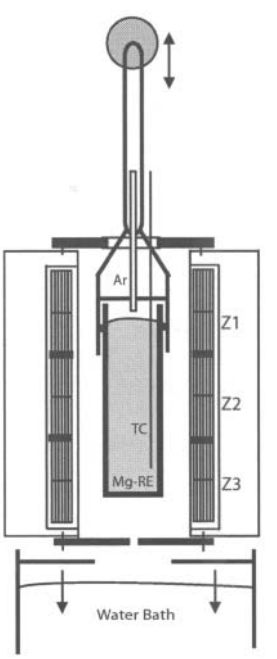

Figure 1: Schematic representation of the three-zones tubular furnace used to produce Mg-RE ingots.

The mould and melt were hold alternatively during 60

min at temperatures of 650°C or 750°C, depending on the experiment. After this holding time, the thermocouple was extracted from the melt and the bottom hatch was opened. A y-axis movement inductor was specially designed in order to achieve different pulling velocities of the mould into a water bath located at about 5 cm below the tubular furnace. The pulling velocity v_p ranged in between 8 to 20 cm/min (this corresponds to a range from 1.33×10^{-3} to 3.33×10^{-3} m/s). The different mould geometries used in this study, i.e., rectangular, insulated and non-insulated pipe-shape, can be observed in Fig. 2. The insulated pipe-shape mould was simply surrounded by an external pipe with an inter-wall spacing of 5 mm. Only the Mg-10wt.%Gd ingots were obtained in the three different geometries, whereas the other two alloys were only processed in the insulated and non-insulated pipe-shape moulds.

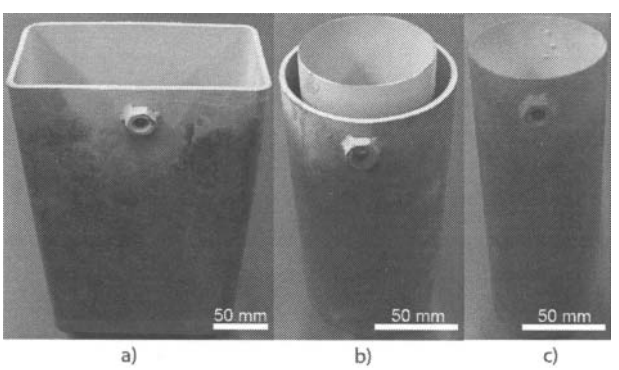

Figure 2: Images of the different mould geometries used in this work: a) rectangular, b) insulated pipe, and c) non-insulated pipe

After solidification, the ingots were extracted from the moulds. The upper and bottom regions of the ingot (about 1.5 cm in length along the main ingot axis) were directly sectioned prior to further analysis of the specimens. In the case of the cylindrical ingots solidified in the insulated and non-insulated pipe-shape moulds, the ingot was sectioned in two halves along its main axis and then sections at 4 different heights were extracted. In order to evaluate the composition homogeneity in the whole volume, chemical analysis was performed by means of an X-ray fluorescense analyzer XRF (Bruker S4explorer) for the Mg-Gd specimens, and through spark emission spectrum analysis in a Spectrolab2003 (Sprectro Analytical Instruments GmbH and Co.) for the Mg-Y and Mg-Nd ingots.

In order to perform macrostructure analyses, a 1 cm thick slice parallel to the main axis of each ingot (rectangular or cylindrical) was extracted. These slices were prepared according to the standard procedure developed by Kree et al. (12), although no etching was necessary to reveal the grain structure of the Mg-10wt.%Gd alloys. In particular the study of the macrostructure in the rectangular Mg-Gd ingots allowed to identify the Columnar-to-Equiaxed Transition (CET) and put it into relation with the solidification conditions.

In order to investigate the texture of the columnar grains observed in some of the specimens, small sections of about 2×2 cm^2 were mechanically polished to mirror quality and then electro-polished in a standard Struers AC2 solution cooled down to -20°C (33 V during 90 s). Then, EBSD measurements were performed in an electron microscope SEM Zeiss Ultra 55.

Results and Discussion

Macrostructure

The macrographs in Fig. 3a, b and c, show the different grain structures observed for each alloy solidified in the insulated pipe-shape permanent moulds. These ingots were solidified by pulling down the mould at 12 cm/min only to contact with the water bath. Then the tubular furnace was shut down while the mould was maintained at this position during 20 min, meaning that except for the bottom 3 cm of the ingot, the rest of the specimen remained inside of the tubular furnace. As the bottom part of the ingot was previously sectioned, only a fully developed columnar region can be observed, i.e., the region containing only equiaxed grains near the chill bottom surface does not appear in the macrographs. In the upper part of the ingot in Fig. 3a, a Columnar to Equiaxed Transition (CET) took place, but the equiaxed grains only occupied the upper 3 cm of the ingot length. The other two alloys did not exhibited a CET. The average chemical composition at different locations in the ingot are indicated in each macrograph. None of the specimens here obtained showed any macrosegregated regions. Below each macrograph, optical micrographs of each alloy can be observed. The Mg-10wt.%Gd alloys exhibit a well-defined dendritic structure, while the other ones, due to low content of solute, present more likely a columnar cellular morphology with some microsegregation channels of a phase rich in Y or Nd in between the cells.

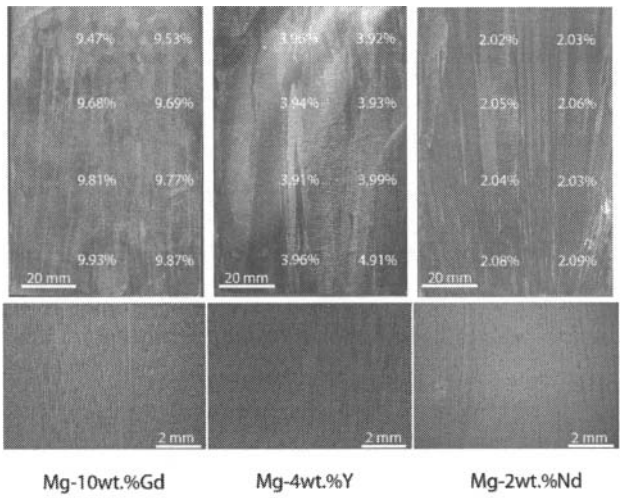

Figure 3: Macro and micrographs of a) Mg-10wt.%Gd, b) Mg-4wt.%Y, and c) Mg-2wt.%Nd alloys solidified in the insulated pipe-shape mould pulled down at v_p = 12 cm/min to contact with the water bath, then cooled down directly in the furnace. The composition measurements at different regions of the ingots are clearly indicated.

Another casting was obtained with the same type of insulated mould, but by keeping v_p constant until the 95% of the ingot volume was inside the water bath. In this case, the CET was present for alloys. This CET occurred much earlier during solidification and relatively big equiaxed grains occupied more than a half of the ingot volume. Indeed, although the external insulation helps to keep the heat inside the mould when it is pulled down to the water bath, the melt temperature still decreases when the ingot is inside the water bath, and therefore equiaxed grains can nucleate ahead of the columnar front. This was confirmed by the macrostructure observed in the ingot solidified in the non-insulated pipe-shape mould pulled down at a speed of 12 cm/min. In this case only in the bottom and near the lateral walls a few columnar grains developed along the first half of the ingot. The rest of the volume was conformed by equiaxed grains.

Further characterization of the grain distribution can be better observed in Fig. 4, which shows the macrostructure observed in Mg-10wt.%Gd alloys solidified in the rectangular mould at different pulling velocities. Due to the symmetry along the vertical axis of the ingot, only a half of a 2D projection of these ingots is shown, in the upper row for the ingots where the initial melt temperature T_{melt} (i.e., before pulling downwards into the water bath) was of 650°C, and in the bottom row for those with T_{melt} = 700°C. The effect of the pulling velocity v_p on the grain orientation with respect to the casting direction can be clearly observed. At the lowest pulling velocity, columnar grains evolve slightly inclined towards the centre of the specimen. This means that the isotherms are nearly perpendicular to the casting direction. As v_p is increased, the depth of the mushy zone increases as one moves towards the centre of the specimen and the isotherms acquire a nearly U-shape. Therefore the columnar grains grow rather towards the centre of the specimen, at an angle α with respect to the mould wall that increases with v_p. In the centre of each of the ingots when $v_p \geq 8$ cm/min, a region containing equiaxed grains can be observed. These grains appeared always slightly larger in a precise direction, along the main axis of the ingot when $v_p \approx 12$ cm/min, perpendicular to it when $v_p \geq 12$ cm/min. The region containing the equiaxed grains is larger in volume as v_p and T_{melt} increase, but the size of these grains gets considerably reduced. The averaged equiaxed grain size ϕ for each specimen is also indicated in Fig. 4.

Texture

The texture of the as-cast specimens was investigated through EBSD measurements performed on the fully developed columnar region of a Mg-10wt.%Gd ingot solidified in the insulated cylindrical mould at an initial pulling speed of 12 cm/min, until the mould bottom made contact with the water bath, and then cooled down inside the tubular furnace. Under these directional solidification conditions, the texture measurement can be directly related to the primary trunk growth direction. Very simply expressed, the probability of finding the dendrite growth direction at an angle θ from the thermal gradient is proportional to a function $\sin\theta$ (10; 11). At the beginning of solidification, in the chill surface, the probability of finding the specific growth direction of a dendrite perfectly aligned with G is small, but it increases to a maximum as the grown distance from the chill also increases. Naturally, the angle between the growth direction and G also decreases to a value near, but different to zero, and the distribution of possible grain orientations around this maximum gets also reduced.

Figure 5b presents a 2×4 mm^2 surface containing

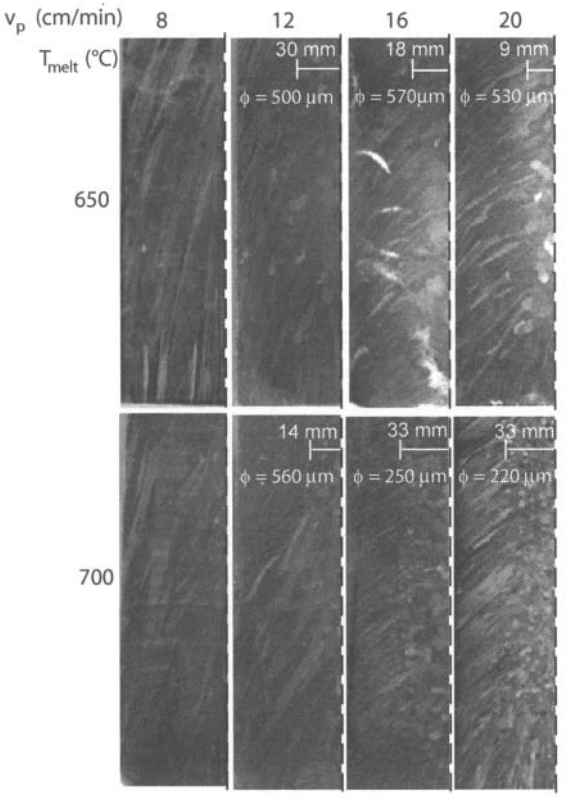

Figure 4: Effect of pulling velocity on the macrostructure of Mg-10wt.%Gd alloys solidified in the rectangular mould. The average equiaxed grain size ϕ is indicated in each ingot.

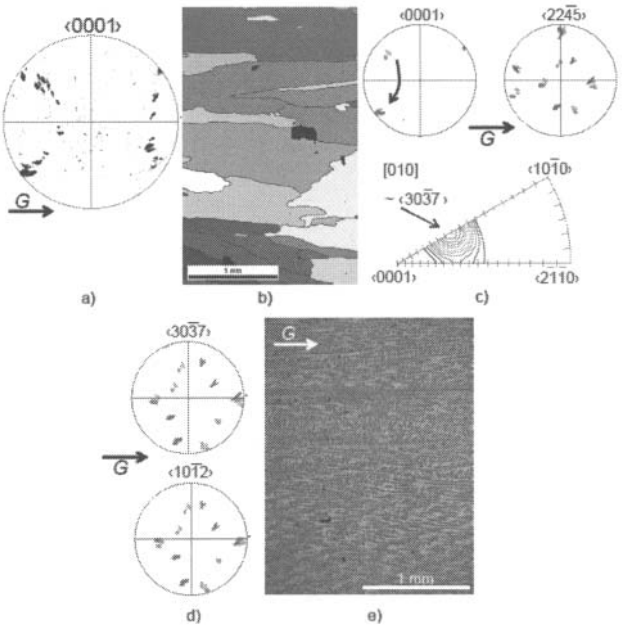

Figure 5: EBSD texture analysis of a directionally solidified Mg-10wt.%Gd alloy. a)⟨0001⟩ pole figure drawn from the crystallographic orientation of the Mg-10wt.%Gd directionally solidified grains shown in b); c) ⟨0001⟩ and ⟨22$\bar{4}$5⟩ pole figures of selected grains (top) and inverse pole figure of the whole analyzed surface (bottom); d) ⟨30$\bar{3}$7⟩ and ⟨10$\bar{1}$2⟩ pole figures of selected grains; e) microstructure of the specimen inside the analyzed surface.

about 20 grains with different crystallographic orientations. Note that the grey shades refer to differences in the crystallographic orientation which will be discussed with respect to the texture below. The coloured grains are marked in order to reveal their specific orientation in the respective pole figure. The ⟨0001⟩ pole figure in Fig. 5a clearly shows that a texture along a well defined direction exists in the grains contained in the examined surface, i.e., the ⟨0001⟩ directions of the crystals in these grains rotate all around a single axis. Due to the distribution of the ⟨0001⟩ directions of the crystals inside these grains, the rotation axis is clearly not lying within the basal plane. This means that the texturization along a ⟨11$\bar{2}$0⟩ direction observed in previous works for Mg-Al alloys is not present in the Mg-Gd system. The pole figures presented in Fig. 5c were drawn to find precisely the rotation axis along which the texture direction could be contained. In order to better perform this analysis, only the orientation of four selected grains are shown. Blue and red grains have similar orientations, different from the also similar dark and light green grains. Therefore only two well localized spots with their corresponding colours can be identified in the ⟨0001⟩ pole figure. The other type of texture reported in literature for Mg-alloys is along ⟨22$\bar{4}$5⟩ directions. In the corresponding ⟨22$\bar{4}$5⟩ pole figure none of the six equivalent directions from each of the selected grains is aligned with the thermal gradient, and actually these are distributed randomly in the pole figure.

In order to identify the crystallographic direction better aligned with G, an inverse pole figure was drawn from the crystallographic orientation of each grain. This is shown in the bottom part of Fig. 5c. The [010] index indicated in the upper-left corner means that the inverse pole figure

was drawn by taking the specimen as seen from a plane perpendicular to the direction of G. A well texturized grain distribution can be identified in this inverse pole figure, with a maximum near to a $\langle 30\bar{3}7 \rangle$ direction. As can be seen in the remaining pole figures of Fig. 5d, the $\langle 30\bar{3}7 \rangle$ and $\langle 10\bar{1}2 \rangle$ directions are almost equivalent. The main texture direction, which should correspond to the dendrite trunk growth direction, has been indicated in these two pole figures. The dendritic microstructure inside the grains analyzed through EBSD can be observed in Fig. 5e. Most of the primary trunks are aligned nearly parallel to G, which confirms the assumption that the texture is a measure of the dendrite trunk growth direction. Nevertheless, it is not possible to make any assumption on the specific secondary arms growth directions, since these are not always lying in the observed section. Further studies of these microstructures through X-ray tomography still need to be performed.

Conclusion

An experimental technique has been developed in order to produce ingots of homogeneous composition and free of porosity and inclusions. A set of parameters were imposed in order to better control the macrostructure. A columnar structure can be obtained when $v_p < 12$ cm/min and the occurrence of the CET can be retarded by stopping the pulling and leaving the specimen to cool down inside the furnace. A well texturized structure along a $\approx \langle 10\bar{1}2 \rangle$ direction develops in directionally solidified Mg-10wt.%Gd alloys. This is different from previous observations on the texture evolution in AZ and AM alloys. The growth of columnar well texturized grains in this binary system is a promising field, in particular for the production of single-grain components made of Mg-alloys.

Acknowledgments

The authors would like to thank Sabine Schubert and Volker Kree for their technical support in the chemical analysis and EBSD measurements, respectively.

References

[1] L.L. Rokhlin. *Magnesium alloys containing rare earth metals.* Taylor and Francis, 2003.

[2] H. Dieringa, N. Hort, and K.U. Kainer. Investigation of minimum creep rates and stress exponents calculated from tensile and compressive creep data of magnesium alloy ae42. *Mat. Sci. and Eng. A*, 510-511:382–386, 2009.

[3] M.A. Gibson, S. Zhu, M.A. Easton, and J.-F. Nie. Microstructure, tensile properties and creep resistance of binary Mg-Rare Earths alloys. *Magnesium Technology*, Edited by S.R. Agnew, N.R. Neelameggham, A. Yberg and W.H. Sillekens:233–238, 2010.

[4] K. Pettersen, O. Lohne, and N. Ryum. Crystallography of directionally solidified magnesium alloy AZ91. *Metall. Mater. Trans.*, 20 A:847–852, 1989.

[5] K. Pettersen, O. Lohne, and N. Ryum. Dendritic solidification of magnesium alloy AZ91. *Metall. Mater. Trans.*, 21A:221–230, 1990.

[6] D. Mirkovic and R. Schmid-Fetzer. Directional solidification of mg-al alloys and microsegregation study of mg alloys az31 and am50: Part ii. comparison between az31 and am50. *Metall. Mater. Trans.*, 40 A:974–980, 2009.

[7] J. Eiken, G. Klaus, D. Mirkovic, I. Steinbach, A. Bührig-Polaczek, and R. Schmid-Fetzer. Numerical and experimental investigation of dendritic growth texture evolution in mg-al alloys with hcp lattice anisotropy. *Modeling of Casting, Welding and Advanced Solidification Processes XII (Edited by S.L. Cockcroft and D.M. Maijer)*, pages 553–560, 2009.

[8] A. Mariaux. *Texture Formation in Hot-Dip Galvanized Coatings: Nucleation and Growth of Anisotropic Grains in a Confined Geometry.* PhD thesis, EPFL No. 4646, 2010.

[9] A. Mariaux, T.-V.-Putte, and M. Rappaz. Modeling nucleation and growth of zinc grains in hot-dip galvanized coatings. *Modellling of Casting, Welding and Advanced Solidification Processes. Edited by S. Crockcroft and D. Maijer*, XII:667–674, 2009.

[10] C.A. Gandin, M. Rappaz, D. West, and B.L. Adams. Grain texture evolution during columnar growth of dendritic alloys. *Metall. Mater. Trans. A*, 26 A:1543–1551, 1995.

[11] F. Gonzales and M. Rappaz. Grain selection and texture evolution in directionally solidified Al-Zn alloys. *Metall. Mater. Trans. A*, 39 A (9):2148–2160, 2008.

[12] V. Kree, J. Bohlen, D. Letzig and K.-U. Kainer. The Metallographical Examination of Magnesium Alloys. *Prakt. Metall.*, 41 (5):233–246, 2004.